9-15-2016

Adsorption of Sodium and Cesium on Aggregates of C60

Martina Harnisch
University of Innsbruck

Matthias Daxner
University of Innsbruck

Paul Scheier
University of Innsbruck

Olof Echt
University of New Hampshire, Olof.Echt@unh.edu

Regular Article

Adsorption of sodium and cesium on aggregates of C_{60}

Martina Harnisch[1], Matthias Daxner[1], Paul Scheier[1], and Olof Echt[1,2,a]

[1] Institut für Ionenphysik und Angewandte Physik, University of Innsbruck, Technikerstrasse 25, 6020 Innsbruck, Austria
[2] Department of Physics, University of New Hampshire, Durham, New Hampshire 03824, USA

Abstract. We explore the formation of C_{60} sodium and C_{60} cesium complexes in superfluid helium nanodroplets. Anomalies in mass spectra of these doped droplets reveal anomalies in the stability of ions. $(C_{60})_m Cs_n^+$ ions ($m \leqslant 6$) are particularly abundant if they contain $n = 6m + 1$ cesium atoms; $(C_{60})_m Cs_n^{2+}$ dications ($m \leqslant 3$ or 5) are abundant if $n = 6m + 2$. These findings are consistent with the notion that alkali metal atoms (A) transfer their valence electrons into the three-fold degenerate lowest unoccupied orbital of C_{60}, resulting in particularly stable $C_{60}A_6$ building blocks. However, $(C_{60})_4 Cs_n^{2+}$ dications display an entirely different pattern; instead of an expected anomaly at $n = 6 \times 4 + 2 = 26$ we observe a strong odd-even alternation starting at $n = 6$. Also surprising is the effect of adding one H_2O or CO_2 molecule to $(C_{60})_m Cs_n$ mono- or dications; anomalies shift by two units as if the impurity were acting as an acceptor for two valence electrons from the alkali metal atoms.

1 Introduction

Two decades ago, Pat Martin's group at the MPI Stuttgart published a series of reports on gas-phase reactions of C_{60}, C_{70}, and their aggregates with metal atoms [1–6]. Fullerene and metal vapor were introduced into cold helium gas; reaction products were extracted into vacuum and multi-photon ionized. Mass spectra of fullerene monomers coated with M = Ca, Sr, or Ba provided evidence for geometric shell structure: magic numbers at $C_{60}M_{32}^+$ and $C_{70}M_{37}^+$ indicated that alkaline-earth metals preferentially adsorb at the center of carbon rings [2,3]. For C_{60} coated with large amounts of calcium, three additional distinct adsorbate layers could be identified.

Complexes of C_{60} and alkali metals (A), on the other hand, showed evidence for electronic shell structure: magic numbers in the ion abundance of $(C_{60})_m A_n^+$ occurred at $n = 6m + 1$, and at $n = 6m + 2$ for $(C_{60})_m A_n^{2+}$ dications [1,3]. $C_{60}A_6$ was interpreted as a building block in which the alkali metal atoms transfer their valence electrons to the three-fold degenerate lowest unoccupied orbital (t_{1u}) of the fullerene, forming essentially ionic bonds. One or two additional A^+ ions are needed to provide for the net charge of the "magic" mono- and dications. However, a different pattern was observed in a later study of C_{60}-potassium complexes by the MPI group [7,8]. By thermalizing the neutral precursors in helium at 900 K, subsequent cooling and soft single-photon ionization the researchers inferred that neutrals with the composition $(C_{60}K_2)_m$ ($m = 2, 3, 4$) are extremely stable.

Theoretical studies of C_{60}-alkali complexes agree with the interpretation of mostly ionic bonding. Chandrakumar and Ghosh [9] report that the charge on a single sodium atom adsorbed on C_{60} derived by the Mulliken method is 0.89. Weis et al. [10] find that the Mulliken charge is >0.90 per potassium atom for $C_{60}K_n$, $n \leqslant 3$; the same holds for $(C_{60})_2 K_n$ for $n \leqslant 6$ [8]. Considering adsorption of up to 12 Li, Na or K atoms on C_{60}, Hamamoto et al. [11] find that the Mulliken charge is smallest for lithium. Wang and Jena [12] conclude that the ground state of $C_{60}Li_6$ corresponds to a configuration in which the Li atoms occupy near-neighbor positions although other configurations with the adsorbate atoms being more uniformly distributed over the surface are nearly degenerate.

The above mentioned features in mass spectra were particularly prominent for A = K and Rb; Li and Na showed more complex patterns. Cs, on the other hand, had the tendency to form metal-rich ions with n extending up to 500; near-threshold single-photon ionization revealed electronic shell closings for $C_{60}Cs_n^+$ at $n = 12, 27, 33, 44, \ldots$ [3,4]. These features were successfully modeled with density-functional theory assuming that the valence electrons of Cs are confined to a spherical shell around the C_{60} core [4,13].

More recently, the search for light-weight materials for hydrogen storage has renewed interest in fullerene-metal complexes [14,15]. In undoped fullerenes, physisorbed hydrogen is bound too weakly while chemisorbed hydrogen is bound too strongly; the adsorption energies are not compatible with the requirement of reversible hydrogen storage and release at ordinary temperatures. Doping fullerenes with alkali or earth alkaline metals

[a] e-mail: olof.echt@unh.edu

promises to elevate adsorption energies to several tenths of an eV [9,12,16]. Experiments have shown that as much as 5 wt% of H_2 could be reversibly adsorbed and desorbed in $C_{60}Li_6$ and $C_{60}Li_{12}$; the storage capacity of $C_{60}Na_6$ and $C_{60}Na_{10}$ was found to be slightly lower [17–21]. Moreover, desorption temperatures were reduced to about 260 °C, well below the temperature at which hydrogen desorbs from pure fulleranes [21].

The present study extends previous work by Martin and coworkers [1–6]. Aggregates of C_{60} and either sodium or cesium are synthesized in superfluid helium nanodroplets and ionized by energetic electrons. Our focus is on singly and doubly charged $(C_{60})_mCs_n$ complexes that include values of n much smaller than considered before [3,4]. In line with previous results for K and Rb we find that $C_{60}Cs_6$ acts as a building block. However, there are noteworthy outliers. One is $(C_{60})_4Cs_n^{2+}$ which shows no propensity for $C_{60}Cs_6$ building blocks but, instead, an odd-even pattern over a wide range of n values. Another system with surprising features are singly and doubly charged $(C_{60})_mCs_n^{z+}$ ions that contain a single H_2O or CO_2 impurity. Here the anomalies are shifted upwards by two units as if the valence electrons from two Cs atoms were transferred to the impurity.

Martin's previous work on $(C_{60})_mNa_n$ was limited to singly charged ions with $m \leqslant 3$ [1,3]. Our present data extend to $m = 10$, and to doubly charged ions. They are consistent with the idea of $C_{60}Na_6$ forming building blocks, but new features emerge in complexes containing many C_{60}.

Fig. 1. Staggered abundance distributions of $(C_{60})_mCs_n^+$. The vertical scale is identical for all data sets but they are vertically offset; individual base lines are indicated. Anomalies (local maxima or abrupt drops in the abundance) occur at $n = 6m + 1$.

2 Experiment and data analysis

Neutral helium nanodroplets were produced by expanding helium (Messer, purity 99.9999%) at a stagnation pressure of 20 bar through a 5 μm nozzle, cooled by a closed-cycle refrigerator to 9.25 K, into a vacuum chamber (base pressure about 4×10^{-6} Pa). Droplets that form in the expansion contain an average number of 4×10^5 helium atoms [22]; the droplets are superfluid with a temperature of 0.37 K [23]. The resulting supersonic beam was skimmed by a 0.8 mm conical skimmer, located 8 mm downstream from the nozzle. The skimmed beam traversed a 20 cm long pick-up region consisting of two separate pick-up chambers [24]. C_{60} (MER, purity 99.9%) was vaporized in the first chamber; metallic sodium or cesium (Sigma Aldrich, purity 99.95% based on a trace metals analysis) were vaporized in the second chamber. The partial vapor pressures of the fullerene and alkali metal were varied in order to obtain the desired ratio of these species in the mass spectra.

The beam emerging from the dual pickup cell was collimated and crossed by an electron beam; its energy was 72 eV. Cations were accelerated into the extraction region of a reflectron time-of-flight mass spectrometer (Tofwerk AG, model HTOF) with a mass resolution $\Delta m/m = 1/5000$ ($\Delta m = $ full-width-at-half-maximum). The base pressure in the mass spectrometer was 10^{-5} Pa. Ions were extracted at 90° into the field-free region of the
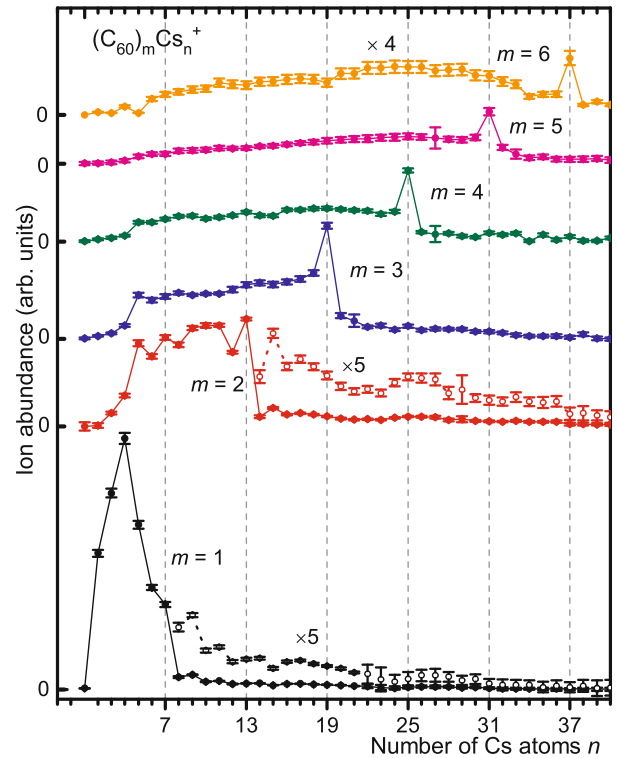
spectrometer by a pulsed voltage. At the end of the field-free region they entered a two-stage reflectron which reflected them towards a microchannel plate detector operated in single ion counting mode. Additional experimental details have been provided elsewhere [25].

Mass spectra were evaluated by means of custom-designed software [26,27]. The routine includes automatic fitting of Gaussians to the mass peaks and subtraction of background by fitting a spline to the background level of the raw data. It explicitly considers the presence of He_n^+, a variety of impurity ions (e.g., OHC_{60}^+) and isotopic patterns. Sodium and cesium are monisotopic. However, the natural abundance of ^{13}C is 1.07%; hence 48% of C_{60} ions have a mass exceeding 720 u. The abundance of ions (i.e. ions of a specific composition, $(C_{60})_mA_n^+$ where A = Na or Cs) is derived by a matrix method.

3 Results

Mass spectra of helium nanodroplets doped with C_{60} and sodium or cesium feature cations containing as many as 10 C_{60} and dozens of alkali atoms. The abundance distributions of $(C_{60})_mCs_n^+$ ions versus n are shown in Figure 1 for $m \leqslant 6$. Data sets are offset vertically; individual base lines are indicated. $C_{60}Cs_n^+$ ions feature a maximum at $n = 4$ and an abrupt drop (by a factor seven) at $n = 7$. For clarity, the abundance of $C_{60}Cs_n^+$, $n \geqslant 8$, is redrawn (dashed
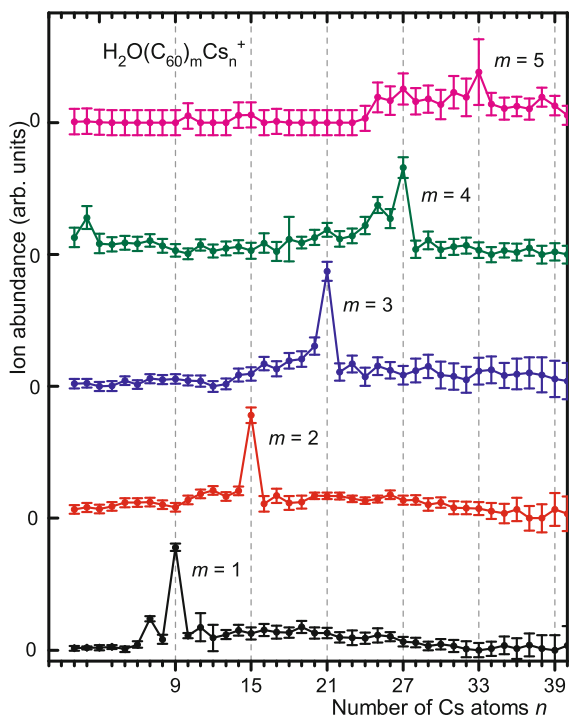
Fig. 2. Staggered abundance distributions of $H_2O(C_{60})_m Cs_n^+$. Maxima occur at $n = 6m + 3$.

Fig. 3. Staggered abundance distributions of $CO_2(C_{60})_m Cs_n^+$. Maxima occur at $n = 6m + 3$.

Fig. 4. Staggered abundance distributions of $(C_{60})_m Cs_n^{2+}$ dications. For $m \leqslant 3$ and $m = 5$ maxima occur at $n = 6m + 2$ but for $m = 4$ the pattern is completely different.

line) after multiplying by a factor 5. The $(C_{60})_2 Cs_n^+$ series features an abrupt (factor 10) drop at $n = 13$. For $m = 3$, 4, 5, 6 maxima followed by steep drops appear at $n = 19$, 25, 31, 37, respectively. In short, for all values of m the ion abundance drops abruptly at $n = 6m + 1$. Here and in the following figures vertical grid lines are drawn to emphasize this periodic pattern.

Figures 2 and 3 present abundance distributions of $H_2O(C_{60})_m Cs_n^+$ and $CO_2(C_{60})_m Cs_n^+$ for $m \leqslant 5$. Maxima followed by abrupt drops occur at $n = 6m + 3$, i.e. they are shifted upward by two units with respect to anomalies in pure $(C_{60})_m Cs_n^+$. Note that the error bars shown in the figures are automatically computed by the fitting routine. In some regions they are much larger than statistical fluctuations; errors are probably overestimated because the routine allows for potential interference with other, unresolved ions.

Distributions of $(C_{60})_m Cs_n^{2+}$ dications are displayed in Figure 4. For $m = 1$, 2, 3, and 5 maxima appear at $n = 6m + 2$[1]. $(C_{60})_4 Cs_n^{2+}$, however, shows an entirely different pattern: instead of the expected maximum at $n = 6 \times 4 + 2$ an odd-even alternation of the abundance commences at $n = 6$ and continues up to at least $n = 46$. The pattern contrasts with the mostly smooth distribution of singly charged $(C_{60})_4 Cs_n^+$ in Figure 1.

Adding a water or carbon dioxide molecule to $(C_{60})_m Cs_n^{2+}$ dications causes the maxima to shift from

---

[1] For $C_{60} Cs_n^{2+}$ the maximum at $n = 9$ is preceded by another one at $n = 7$. Several other ion series show such a secondary maximum preceding the main one by two units (see e.g. Figs. 2 and 6).
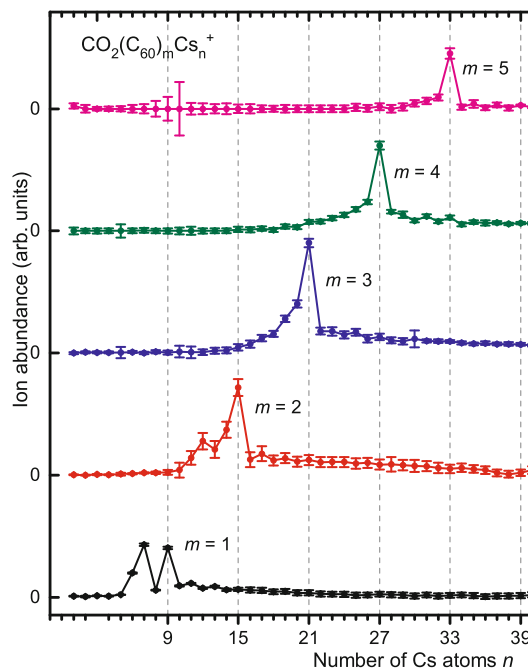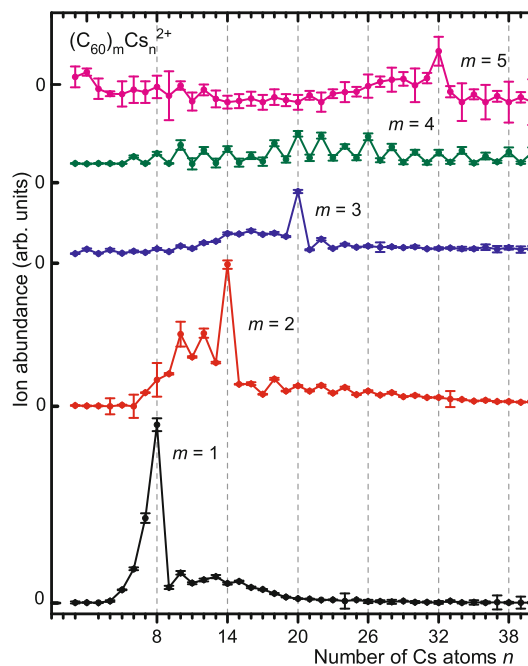
$n = 6m + 2$ to $n = 6m + 4$ (see Fig. 5). Furthermore, pronounced odd-even alternations appear in the distributions of $H_2O(C_{60})_m Cs_n^{2+}$.

So far we have displayed ion abundances on linear scales. However, the ion abundance of $(C_{60})_m Na_n$ cations and dications tends to decline rather steeply as n increases. In this situation, local anomalies are revealed
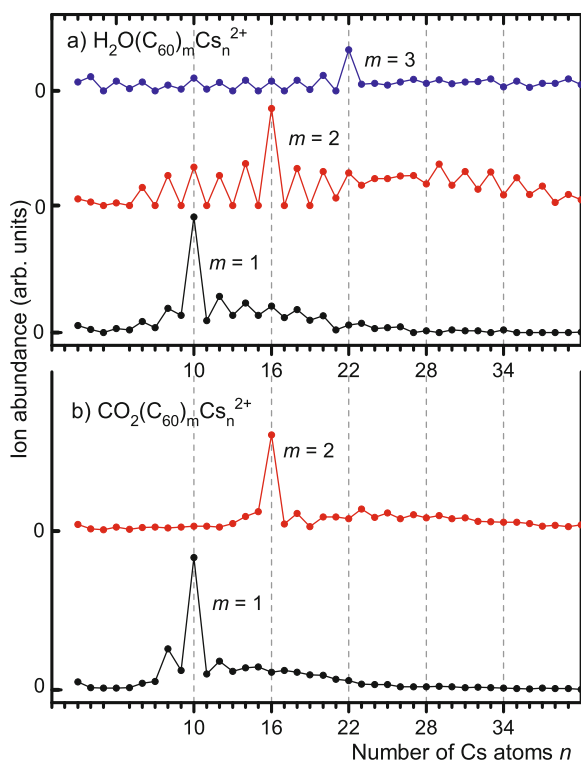
Fig. 5. Staggered abundance distributions of $H_2O(C_{60})_m Cs_n^{2+}$ and $CO_2(C_{60})_m Cs_n^{2+}$ dications (panels a and b, respectively). Maxima occur at $n = 6m + 4$.

more clearly if the distribution is divided by a smooth envelope function which we compute from local averages of the experimental ion abundance with Gaussian weighting [28]. By definition, these relative ion abundances average to 1. Figure 6 reveals that the relative ion abundances of $(C_{60})_m Na_n^+$, $m \leqslant 5$, exhibit an abrupt onset of odd-even oscillation at $n = 6m + 1$. The oscillations are extremely strong; for $C_{60}Na_n^+$ the abundance ratio of adjacent odd- and even-numbered ions is about 15:1. A broad minimum around $n = 5$ is also noteworthy. It occurs for all values of m but is more distinct in the original abundance distributions, i.e. before dividing by a smooth envelope function.

The ion abundance of $(C_{60})_m Na_n^+$ has been recorded for fullerene aggregates as large as $m = 10$, see Figure 7. The broad minimum around $n = 5$ is common to all values of m. Another noteworthy feature is a local maximum at $n = 14$ which occurs for $5 \leqslant m \leqslant 10$. The occurrence of odd-even oscillations beyond $n = 6m + 1$ cannot be confirmed because of insufficient data quality in this size range.

For $(C_{60})_m Na_n^{2+}$ dications the oscillations commence at $n = 6m + 2$ (see Fig. 8). Data are not shown for $m = 4$ because they are marred by interference with other ions.

4 Discussion

We have identified anomalies (local maxima or abrupt drops) in the abundance distributions of fullerene-cesium
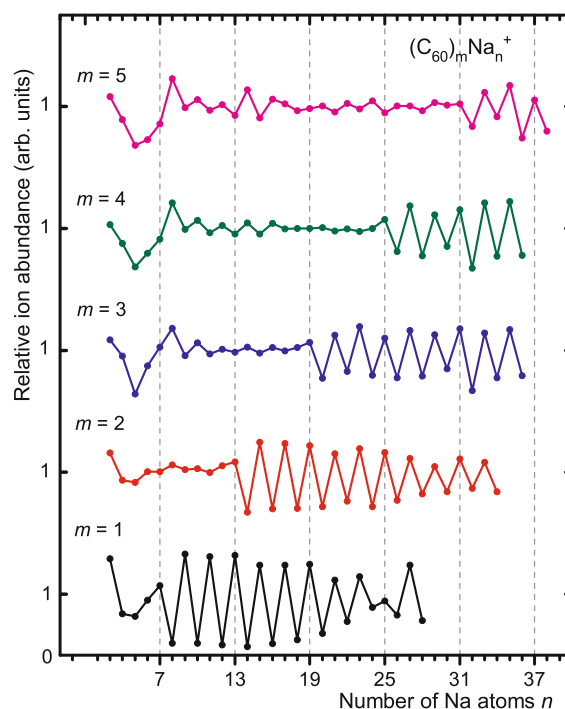
Fig. 6. Staggered abundance distributions of $(C_{60})_m Na_n^+$. Odd-even oscillations commence at $n = 6m + 1$.

Fig. 7. Staggered abundance distributions of $(C_{60})_m Na_n^+$, $6 \leqslant m \leqslant 10$.

complexes. What do these anomalies tell us? Growth of neutral clusters in helium droplets is a statistical process. The size distribution of neutral aggregates is featureless because the probability of capture does not depend on the stability of the complex that is formed. Anomalies

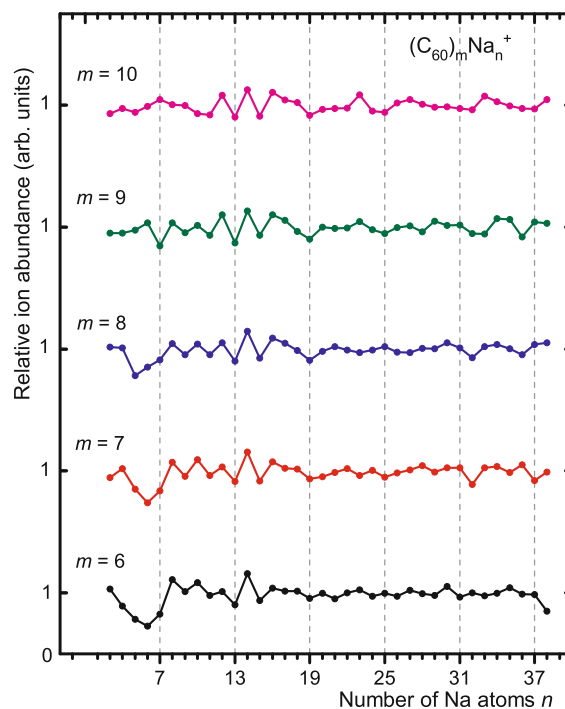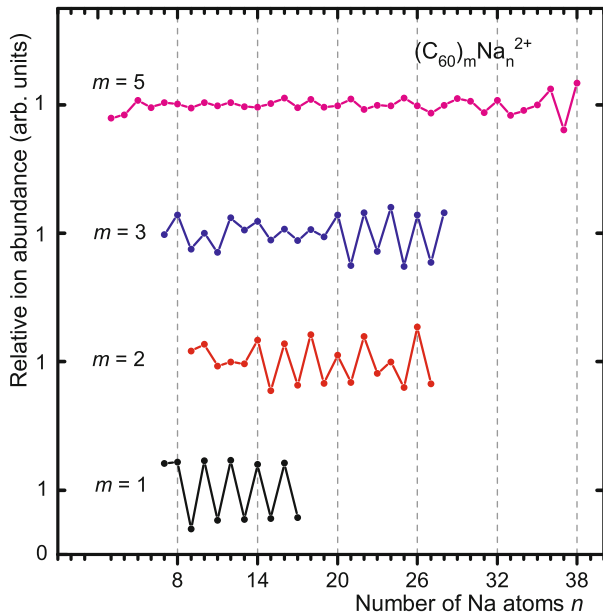**Fig. 8.** Staggered abundance distributions of $(C_{60})_m Na_n^{2+}$. Odd-even oscillations commence at $n = 6m + 2$. Data for $(C_{60})_4 Na_n^{2+}$ are not shown because they are marred by interference with other ions.

in the abundance of cluster ions arise from fragmentation upon ionization[2]. Vibrationally excited ions that feature energetically facile dissociation channels (low dissociation energies D_n) are less likely to survive on the time scale of mass spectrometric analysis than strongly bound ions. Thus the maxima and abrupt drops in the abundance distributions reveal ions that are exceptionally stable with respect to monomer loss, relative to the next larger cluster. The method by which neutral precursors are formed may have some effect on the overall distribution of the ions, but not on local anomalies.

With one exception, namely $(C_{60})_4 Cs_n^{2+}$, abundance distributions of $(C_{60})_m Cs_n^{z+}$ ($z = 1, 2$) feature local maxima (or abrupt drops) at $n = 6m + z$. In previous work, Martin and coworkers produced fullerene-alkali complexes in a gas aggregation source and formed mono- and dications using a pulsed excimer (with wavelengths of 248, 193 or 157 nm) or dye laser [1,3]. One-photon near-threshold ionization led to featureless abundance distributions of

$(C_{60})_m A_n^+$. However, at high fluence, when the laser would not only ionize but also heat the cluster ions, anomalies were observed consistent with the $n = 6m + z$ rule for $(C_{60})_m K_n^+$ ($m \leqslant 3$), $(C_{60})_m K_n^{2+}$ ($m = 3, 5$), $(C_{60})_m Rb_n^+$ ($m \leqslant 6$), and $(C_{60})_m Rb_n^{2+}$ ($m = 3, 5, 7$). Dications with an even number of alkalis were not identified even though the mass resolution was four times better than ours[3]. Martin and coworkers proposed that for K- and Rb doped fullerenes[4] the first few alkali atoms bind ionically by transferring their valence electrons to the lowest unoccupied orbital of C_{60} which is three-fold degenerate, thus explaining the $n = 6m + z$ rule. Our data demonstrate that cesium behaves similar to potassium and rubidium.

On the other hand, fullerenes doped with lighter alkali metal atoms show deviations from this pattern. The abundance distributions of $(C_{60})_m Na_n^{z+}$ ($z = 1, 2$, see Figs. 6 and 8) changes abruptly at $n = 6m + z$, from smooth to an alternating odd-even pattern, but there is no evidence for enhanced stability of $(C_{60}Na_6)_m Na^+$ or $(C_{60}Na_6)_m Na_2^{2+}$. Spectra of $C_{60}Li_n^{z+}$ with $z = 1, 2$ show a feature at $n = 6 + z$, but a more prominent feature indicates special stability of $C_{60}Li_{12}^{z+}$ regardless of its charge z [3].

For additional insight we now turn to other reports. Theoretical work has been limited so far to the lighter alkalis (with the exception of jellium-type calculations for C_{60} fully coated with one or more layers of cesium [4,13], and recent calculations restricted to Cs monomer and dimers [33,34]). These studies reveal a delicate balance between Coulomb repulsion between atomic ions favoring uniform coverage, and metallic bonding favoring island formation [35]. Density functional theory studies of $C_{60}A$ (A = Li, Na, K) generally find that an alkali atom preferentially adsorbs at a hexagonal site [36–38] (note that some studies mentioned here refer to complexes with a net charge of $+e$ or $-e$). For $C_{60}Li$, however, the energy differences between hexagonal and pentagonal sites are very small; Hamamoto et al. [11], Wang and Jena [12] and Sun et al. [39] report a small energetic preference for the pentagonal site. The degree of charge transfer increases in the order Li/Na/K [11,37,40].

For $C_{60}Li_6$ there is general agreement that the adatoms reside at pentagonal sites that are as close together as possible. In other words, the adatoms decorate a hemisphere of C_{60} [11,12,37]. For $C_{60}Na_6$ and $C_{60}K_6$, on the other hand, it is found that adatoms preferentially bind to hexagonal sites and stay away from each other as far as possible [8,36,37,41][5].

---

[2] In our work, nascent ions are highly excited. There are several pathways for formation of cations by electron ionization of doped helium droplets. One involves He$^+$ formation followed by resonant hole hopping and charge transfer with the dopant which releases approximately the difference between the ionization energy of helium (24.59 eV) and the dopant C_{60} (7.60 eV) or Cs (3.89 eV) [29,30]. Other mechanisms, particularly effective for heliophobic dopants, involve highly mobile He*$^-$ or Penning ionization by metastable He* which release similarly large excess energies [30,31]. Neutral cesium clusters are expected to reside on the surface of helium nanodroplets [32]. However, the addition of C_{60} which is electrophilic and highly polarizable will induce Cs_n clusters to dissolve in the droplet provided $n > 1$ [33].

[3] The authors stated that "(each peak of dications) with an even number of fullerenes coincides with a singly ionized peak", but this is not quite correct if one analyzes ions that contain an odd number of ^{13}C atoms. Martin and coworkers merely published unprocessed global mass spectra, therefore details cannot be assessed.

[4] The only cesium data that Martin and coworkers published showed C_{60}^+ decorated with more than 40 adsorbed cesium atoms [4].

[5] Formally, the six adatoms form two trimers on opposite sides of C_{60} in a configuration commonly referred to as 2h3.

12 Li atoms uniformly cover C_{60} in a configuration of icosahedral symmetry, with all pentagonal sites being decorated [11,37,41,42]. 12 Na atoms, on the other hand, prefer to form three islands of four atoms each [37]. Each island consists of an approximately equilateral trimer (with two atoms at pentagonal sites and one at a hexagonal site); the forth atom caps the trimer. The same structure is found for $C_{60}K_{12}$ [43]. The degree of charge transfer in $C_{60}K_{12}$ appears to be slightly less than for $C_{60}Na_{12}$ and much less than for $C_{60}Li_{12}$ [43], which is opposite to the trend for charge transfer in $C_{60}A$.

Few theoretical studies have considered alkali adsorption on C_{60} aggregates. Hernandez-Rojas et al. [44] have calculated optimum adsorption sites of Li^+, Na^+ and K^+ on $(C_{60})_m$ with $m \leqslant 13$. Li^+ prefers triangular interstitial sites whereas Na^+ and K^+ prefer tetrahedral sites. Zurek et al. [8] find that the adatoms in $(C_{60})_2K_4$ reside in the groove between the two C_{60}. Apparently the enhanced adsorption energy at groove sites [45] outweighs the tendency for ions to spread out uniformly due to Coulomb repulsion. However, two K atoms added to $(C_{60})_2K_4$ will reside at opposite ends of the C_{60} dimer, on the molecular axis [8].

Photoelectron spectra of $C_{60}K_n$ ($n \leqslant 3$) indicate essentially ionic bonding [46]. Spectra of $C_{60}Na_n^-$ ($n \leqslant 12$), however, suggest that sodium atoms on C_{60} tend to form trimers or perhaps tetrahedral tetramers rather than uniformly covering C_{60} as expected if Coulomb repulsion between the adsorbed cations would prevail [47–49], in agreement with the theoretical work mentioned above [37].

The quantity that is most relevant for a comparison with abundance distributions is the dissociation energy D_n for the reaction

$$(C_{60})_m Cs_n^{z+} = (C_{60})_m Cs_{n-1}^{z+} + Cs - D_n. \qquad (1)$$
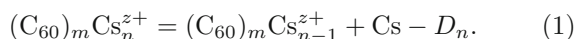
For example, the abundance distribution of $ArHe_n^+$ which reveals three anomalies [50] is in striking agreement with computed dissociation energies [51]. Unfortunately, the only system for which energies of $(C_{60})_m Cs_n^{z+}$ have been computed versus a continuous range of n values, thus allowing the extraction of D_n values, is $C_{60}Li_n^{z+}$ with $z = 0$, 1, 2, and $n \leqslant 14$ [3]. The authors performed semiempirical quantum chemical calculations using the MNDO method; simulated abundance distributions using the Monte Carlo approach were in good agreement with experimental data. However, as mentioned above, lithium-doped fullerenes are not representative of fullerenes doped with heavier alkali atoms. Chandrakumar and Gosh have applied density functional theory to compute energies of $C_{60}Na_n$ for $n = 1, 2, 8$ and find that the average binding energies of the alkalis remain almost constant [9], but this result says nothing about the possible existence of an anomaly at D_6.

Furthermore, theoretical work reported so far is unable to reveal the origin of odd-even oscillations in some abundance distributions of fullerene-alkali complexes that appear beyond $n = 6m + z$. Odd-even alternations appear in experimental abundance distributions and ionization energies of most monovalent simple metal clusters; they also appear in computed ionization energies, electron affinities, dissociation energies and other proper-

ties [52] (for experimental and theoretical data pertaining to Cs_n clusters see [53,54]). Odd-even alternations are often interpreted to indicate metallic bonding [1]; within an electronic jellium model they arise as a result of triaxial shape deformations [52,55]. Thus, the sudden appearance of odd-even oscillations in the distributions of $(C_{60})_m Na_n^{z+}$ beyond $n = 6m + z$ (see Figs. 6 and 8) may indicate a change in the character of chemical bonding in the adsorbate layer [1]. In later work, however, Martin and coworkers [3] proposed an alternative model. They suggested that beyond $n = 6 + 1$ additional Na atoms might successively attach to the seven ionically bound Na in pairs of two, forming Na trimers. Every time such a stable trimer, each containing two metal valence electrons, is completed, a strong peak is observed in the spectrum, resulting in an even-odd alternation. However, this hypothesis would predict the disappearance of odd-even oscillations beyond $n = 3(6 + 1) = 21$ which is at variance with experiment (see Fig. 6). The hypothesis is also at variance with the above-mentioned DFT study of $C_{60}Na_{12}$ which reveals a preference for three sodium tetramers [37].

The pronounced odd-even oscillation in the abundance distribution of $(C_{60})_4 Cs_n^{2+}$ for $6 \leqslant n \leqslant 40$ and the absence of a feature at $n = 6m + 2 = 26$ poses an even greater challenge. Why does this pattern appear when the charge state of $(C_{60})_4 Cs_n^{z+}$ ions is changed from $z = 1$ to 2 or, alternatively, when the number of C_{60} units in $(C_{60})_m Cs_n^{2+}$ increases from $m = 3$ to 4? It is conceivable that large fullerene complexes offer nucleation sites not found for C_{60} or small $(C_{60})_m$ complexes that favor formation of a metallic droplet [44]. Dimple sites offer enhanced adsorption energies for physisorbed molecules [56,57]. But dimple sites exist for all $(C_{60})_m$ complexes with $m \geqslant 3$; what is special about $m = 4$? Calculations will be needed to better understand the structure and nature of chemical bonding in these species.

Our understanding is also challenged by the intriguing change that occurs when one analyzes mono- and dications that contain an H_2O or CO_2 impurity (see Figs. 2, 3, and 5). Now anomalies appear at $n = 6m+z+2$, i.e. shifted upwards by two units relative to pure $(C_{60})_m Cs_n^{z+}$. A naive interpretation would be that two additional cesium atoms are ionically bound because their valence electrons are transferred to the adsorbed impurity. Such an effect, i.e. a shift of anomalies by two units, has been reported for bare alkali metal clusters containing O_2 or SO_2 impurities [58,59]. However, those molecules feature large adiabatic electron affinities (0.45 and 1.1 eV, respectively [60]) whereas isolated H_2O and CO_2 do not bind an electron.

A more reasonable explanation is a reaction of the impurity with cesium. For water, the reaction would produce $CsOH + CsH$, or

$$H_2O\,(C_{60})_m Cs_n^+ \rightarrow CsOHCsH\,(C_{60})_m Cs_{n-2}^+. \qquad (2)$$

The reaction would shift the anomalies upward by two units because two cesium atoms become unavailable for electron transfer to C_{60}. A related shift has been reported for abundance distributions of sodium clusters upon reaction with SF_6 to form NaF [61]. Furthermore,

mass spectrometric evidence has been reported for efficient chemical reaction of bare cesium clusters with H_2O in helium droplets [62]. However, it is not clear how CO_2 would react to passivate two cesium atoms. Computations are called for to unravel the details.

5 Conclusions

We have interpreted abundance anomalies in mass spectra of helium nanodroplets doped with C_{60} and either sodium or cesium. Cesium-doping results in features similar to those reported previously for fullerenes doped with potassium or rubidium [1,3]; they are consistent with a model involving ionic bonding of up to $n = 6m + z$ Cs atoms in $(C_{60})_m Cs_n^{z+}$ with $z = 1$ or 2 and $m \leqslant 6$. However, adding a H_2O or CO_2 impurity shifts the features upwards as if the impurity were to passivate two cesium atoms. Furthermore, $(C_{60})_4 Cs_n^{2+}$ shows a distinctly different pattern. Hopefully, these unexpected findings will stimulate theoretical work.

References

1. T.P. Martin, N. Malinowski, U. Zimmermann, U. Näher, H. Schaber, J. Chem. Phys. **99**, 4210 (1993)
2. U. Zimmermann, N. Malinowski, U. Näher, S. Frank, T.P. Martin, Phys. Rev. Lett. **72**, 3542 (1994)
3. U. Zimmermann, N. Malinowski, A. Burkhardt, T.P. Martin, Carbon **33**, 995 (1995)
4. M. Springborg, S. Satpathy, N. Malinowski, U. Zimmermann, T.P. Martin, Phys. Rev. Lett. **77**, 1127 (1996)
5. S. Frank, N. Malinowski, F. Tast, M. Heinebrodt, I.M.L. Billas, T.P. Martin, Z. Phys. D **40**, 250 (1997)
6. F. Tast, N. Malinowski, S. Frank, M. Heinebrodt, I.M.L. Billas, T.P. Martin, Z. Phys. D **40**, 351 (1997)
7. A. Enders, N. Malinowski, D. Ievlev, E. Zurek, J. Autschbach, K. Kern, J. Chem. Phys. **125**, 191102 (2006)
8. E. Zurek, J. Autschbach, N. Malinowski, A. Enders, K. Kern, ACS Nano **2**, 1000 (2008)
9. K.R.S. Chandrakumar, S.K. Ghosh, Nano Lett. **8**, 13 (2008)
10. P. Weis, R.D. Beck, G. Bräuchle, M.M. Kappes, J. Chem. Phys. **100**, 5684 (1994)
11. N. Hamamoto, J. Jitsukawa, C. Satoko, Eur. Phys. J. D **19**, 211 (2002)
12. Q. Wang, P. Jena, J. Phys. Chem. Lett. **3**, 1084 (2012)
13. M. Springborg, J. Phys.: Condens. Matter **11**, 1 (1999)
14. P. Jena, J. Phys. Chem. Lett. **2**, 206 (2011)
15. N. Park, K. Choi, J. Hwang, D.W. Kim, D.O. Kim, J. Ihm, Proc. Natl. Acad. Sci. USA **109**, 19893 (2012)
16. M. Yoon, S.Y. Yang, C. Hicke, E. Wang, D. Geohegan, Z.Y. Zhang, Phys. Rev. Lett. **100**, 206806 (2008)
17. P. Mauron et al., Int. J. Hydrogen Energy **37**, 14307 (2012)
18. A. Paolone et al., J. Phys. Chem. C **116**, 16365 (2012)
19. J.A. Teprovich, D.A. Knight, B. Peters, R. Zidan, J. Alloys Compounds **580**, S364 (2013)
20. P.A. Ward, J.A. Teprovich, R.N. Compton, V. Schwartz, G.M. Veith, R. Zidan, Int. J. Hydrogen Energy **40**, 2710 (2015)
21. P. Mauron, M. Gaboardi, D. Pontiroli, A. Remhof, M. Ricco, A. Züttel, J. Phys. Chem. C **119**, 1714 (2015)
22. E.L. Knuth, U. Henne, J.P. Toennies, in *20th Int. Symp. Rarefied Gas Dynamics, Beijing, 1996*, edited by C. Shen (Peking University Press, Beijing, 1997), Vol. 871, ISBN: 9787301033524
23. J.P. Toennies, A.F. Vilesov, Angew. Chemie (Int. Ed.) **43**, 2622 (2004)
24. C. Leidlmair, P. Bartl, H. Schöbel, S. Denifl, M. Probst, P. Scheier, O. Echt, Astrophys. J. Lett. **738**, L4 (2011)
25. H. Schöbel, P. Bartl, C. Leidlmair, S. Denifl, O. Echt, T.D. Märk, P. Scheier, Eur. Phys. J. D **63**, 209 (2011)
26. A. Kaiser et al., J. Chem. Phys. **138**, 074311 (2013)
27. S. Ralser, J. Postler, M. Harnisch, A.M. Ellis, P. Scheier, Int. J. Mass Spectrom. **379**, 194 (2015)
28. S. Prasalovich, K. Hansen, M. Kjellberg, V.N. Popok, E.E.B. Campbell, J. Chem. Phys. **123**, 084317 (2005)
29. A.M. Ellis, S.F. Yang, Phys. Rev. A **76**, 032714 (2007)
30. A. Mauracher et al., Phys. Rep. submitted (2016)
31. S.E. Huber, A. Mauracher, Mol. Phys. **112**, 794 (2014)
32. C. Stark, V.V. Kresin, Phys. Rev. B **81**, 085401 (2010)
33. M. Renzler, J. Postler, A. Hauser, W.E. Ernst, A. Lindinger, R. Zillich, P. Scheier, A.M. Ellis, submitted (2016)
34. A. Kaiser, M. Renzler, L. Kranabetter, M. Schwärzler, R. Parajuli, O. Echt, P. Scheier, Int. J. Hydrogen Energy, submitted (2016)
35. P. Karamanis, C. Pouchan, J. Phys. Chem. C **116**, 11808 (2012)
36. J. Roques, F. Calvo, F. Spiegelman, C. Mijoule, Phys. Rev. Lett. **90**, 075505 (2003)
37. F. Rabilloud, J. Phys. Chem. A **114**, 7241 (2010)
38. M. Robledo, F. Martin, M. Alcami, S. Diaz-Tendero, Theor. Chem. Acc. **132**, 1346 (2013)
39. Q. Sun, Q. Wang, P. Jena, Appl. Phys. Lett. **94**, 013111 (2009)
40. M. Robledo, N.F. Aguirre, S. Diaz-Tendero, F. Martin, M. Alcami, RSC Advances **4**, 53010 (2014)
41. F. Rabilloud, Phys. Chem. Chem. Phys. **16**, 22399 (2014)
42. Q. Sun, P. Jena, Q. Wang, M. Marquez, J. Am. Chem. Soc. **128**, 9741 (2006)
43. F. Rabilloud, Comput. Theor. Chem. **964**, 213 (2011)
44. J. Hernandez-Rojas, J. Breton, J.M.G. Llorente, D.J. Wales, J. Chem. Phys. **121**, 12315 (2004)
45. S. Zöttl et al., Carbon **69**, 206 (2014)
46. L.S. Wang, O. Chesnovsky, R.E. Smalley, J.P. Carpenter, S.J. Hwu, J. Chem. Phys. **96**, 4028 (1992)
47. B. Palpant, A. Otake, F. Hayakawa, Y. Negishi, G.H. Lee, A. Nakajima, K. Kaya, Phys. Rev. B **60**, 4509 (1999)
48. B. Palpant et al., J. Chem. Phys. **114**, 8459 (2001)
49. H.B. Wang, S.J. Li, S.L. Xiu, L. Gong, G. Chen, H. Mizuseki, Y. Kawazoe, J. Chem. Phys. **136**, 174314 (2012)
50. P. Bartl, C. Leidlmair, S. Denifl, P. Scheier, O. Echt, J. Phys. Chem. A **118**, 8050 (2014)
51. F. Tramonto, P. Salvestrini, M. Nava, D.E. Galli, J. Low Temp. Phys. **180**, 29 (2015)
52. M. Brack, Rev. Mod. Phys. **65**, 677 (1993)
53. H.G. Limberger, T.P. Martin, J. Chem. Phys. **90**, 2979 (1989)

54. M. Ali, D.K. Maity, D. Das, T. Mukherjee, J. Chem. Phys. **124**, 024325 (2006)
55. C. Yannouleas, U. Landman, Phys. Rev. B **51**, 1902 (1995)
56. A. Kaiser et al., ChemSusChem **6**, 1235 (2013)
57. O. Echt, A. Kaiser, S. Zöttl, A. Mauracher, S. Denifl, P. Scheier, ChemPlusChem **78**, 910 (2013)
58. H. Göhlich, T. Lange, T. Bergmann, T.P. Martin, Phys. Rev. Lett. **65**, 748 (1990)
59. H. Göhlich, T. Lange, T. Bergmann, T.P. Martin, Z. Phys. D **19**, 117 (1991)
60. NIST Chemistry webbook, http://webbook.nist.gov/chemistry/, accessed July 1, 2016
61. M. Daxner, S. Denifl, P. Scheier, A.M. Ellis, Angew. Chem. (Int. Ed.) **53**, 13528 (2014)
62. S. Müller, S. Krapf, T. Koslowski, M. Mudrich, F. Stienkemeier, Phys. Rev. Lett. **102**, 183401 (2009)